Pergamon

Geochimica et Cosmochimica Acta, Vol. 64, No. 16, pp. 2863–2878, 2000

0016-7037/00 $20.00 + .00

PII S0016-7037(00)00389-6

Trace element partitioning between plagioclase and melt: Investigation of dopant influence on partition behavior

ILYA N. BINDEMAN[1,*] and ANDREW M. DAVIS[2]

[1]Department of Geology & Geophysics, University of Wisconsin, Madison, Wisconsin 53706, USA
[2]Enrico Fermi Institute and Department of Geophysical Sciences, University of Chicago, Chicago, Illinois 60637, USA

(*Received March* 26, 1999; *accepted in revised form March* 13, 2000)

Abstract—We present results from an ion microprobe study of REE-doped and natural concentration plagioclase-basalt run products of Drake (1972) that carries on from our earlier study (Bindeman et al., 1998). The goals of this work are (1) to determine plagioclase/melt partition coefficients for all REE for four analyzed plagioclase compositions (An_{40-80}); and (2) to determine whether doping with REE influences partition coefficients of other REE and other trace elements. In combination with our analyses of Sr-doped runs (Bindeman et al., 1998), the new data allow us to compare partition coefficients (D_ι's) of trace elements at natural concentrations with those in REE-doped and Sr-doped runs. In these comparisons, runs have the same run temperature and compositions, but different doping element(s).

We find that $\ln(D_{REE})$ decreases as a linear function of REE atomic number, in contrast to most plagioclase-melt partition experiments. The slopes of the $\ln(D_\iota)$ vs. %An and RT $\ln(D_\iota)$ vs. %An dependencies of REE and monovalent and divalent cations increase from smaller to larger ions of each valence group. D_{La}/D_Y and D_{La}/D_{Lu} increase by more than 5 times as plagioclase composition changes from An_{80} to An_{40}. Within each valence group, slopes on $\ln(D_\iota)$ vs. %An and RT $\ln(D_\iota)$ vs. %An plots increase linearly with ionic radius, with the trivalent REE showing the steepest slope vs. ionic radius dependence. Application of the elastic modulus model of Blundy and Wood (1994) to our results yielded good results, confirming that elastic properties determine partition behavior. We also present D_ι's for U.

We find no detectable effects of trace element doping on D_ι's of 30 trace elements of varying size and charge. This implies that coupling between different trace elements is not a significant process during partitioning in *natural* systems, even for the case of heterovalent substitutions (such as REE). However, D_{REE} and D_Y in REE-doped runs are 30–100% higher than D_{REE} in undoped runs and Sr-doped runs. Doping with thousands of ppm of three selected REE (it does not matter which three) affects D_ι's of Y and all REE in these runs, including those at natural concentration levels. We suggest that substituting trace cations largely compete for sites of substitution with the mineral-forming cations Na and Ca. We speculate that lower D_{REE} in REE-doped runs are the result of a change in the REE substitution mechanisms at doped concentrations of all REE which leads to a different value of the Henry's law constant. *Copyright © 2000 Elsevier Science Ltd*

1. INTRODUCTION

Trace element partition coefficients (D_ι's) are important in characterizing and modeling primary and evolving terrestrial and extraterrestrial melts based on the trace element compositions of igneous minerals and the melts they were in equilibrium with when they crystallized. A key concern in partitioning studies is the influence of trace element concentration on D_ι's (non-Henry's Law behavior), as trace elements are often doped to wt.% levels in experiments. Doping was necessary to make ion or electron microprobe measurements easier (or possible), especially in earlier studies. In addition, the dependence of D_ι's on trace element concentration must be known when comparing natural systems with strongly differing trace element contents (e.g., tholeiites vs. pegmatites).

Another potentially important aspect of partitioning studies is maintaining charge neutrality. Doping with trace elements of different charge (or oxidation state) may change the coupled substitution mechanism(s) that maintains charge balance. Several possible exchange reactions have been proposed for intracrystalline REE^{3+} charge compensation in feldspars, clinopyroxenes and other common silicates (Kneip and Liebau, 1994; D'Arco and Piriou, 1989; see Discussion below).

The formation of clusters within crystal structures that results from coupled substitution (e.g., Navrotsky, 1978) may complicate concentration dependence of partition coefficients. In addition, the issue of defect equilibria at low (natural) concentration levels in experiments and nature has received much attention and remains controversial (see Drake and Holloway, 1978; Watson, 1985; Beattie, 1993; and Urusov and Dudnikova, 1998 for reviews). Higher values of the Henry's constant and partition coefficients at low concentrations have been attributed to partitioning into defect sites in minerals. In most of these experiments one or a few REE were added to a chemically pure system and a departure from Henry's law behavior was observed. Harrison and Wood (1980) have shown that Henry's law fails at ~1 ppm for garnet-melt REE partitioning. Hoover (1978) showed it for Sm and Tm partitioning between plagioclase and melt. Urusov and Dudnikova (1998) have presented compelling evidence for "trapping effects" of microimpurities in nonsilicate and, more recently, silicate systems (see Urusov and Kravchuk, 1978; Urusov and Dudnikova, 1998).

Recently, Beattie (1993; 1994) argued that there is insuffi-

* Author to whom correspondence should be addressed.

Table 1. Experimental conditions and products of REE-doped and undoped runs.[a]

Run	T (K)	System	Doped element	%An, avg%	Total REE (ppm) Plag	Glass
Undoped						
99-1	1460	MP1 + 20%Ab		51.3	16	88
100-1	1530	MP1 + 10%An		69.2	22	86
101-1	1570	MP1 + 40%An		71.3	7	50
REE-doped						
94-7	1426	MP1 + 50%Ab	La	44.7	6633	25,263
99-7	1460	MP1 + 20%Ab	Nd, Dy, Er	53.0	1208	31,155
99-2	1460	MP1 + 20%Ab	Sm, Eu, Gd	53.0	2368	39,810
99-5	1460	MP1 + 20%Ab	La, Ce, Y, Lu	52.5	3053	25,867
100-4	1530	MP1 + 10%An	La, Ce, Y, Lu	67.7	2899	37,267
100-6	1530	MP1 + 10%An	Nd, Dy, Er	68.5	729	19,041
101-4	1572	MP1 + 40%An	La, Ce, Y, Lu	75.5	2443	38,709
101-3	1572	MP1 + 40%An	Sm, Eu, Gd	75.0	3439	56,373
101-7	1572	MP1 + 40%An	Nd, Dy, Er	75.0	882	16,601

[a] MP1 is a natural basaltic andesite from Mountain Pass, Oregon; Ab and An are synthetic albite and anorthite. %An was measured on the University of Chicago electron microprobe. Added REE are the sum of indicated doped REE. Total ion microprobe-measured REE in undoped runs are the sum of La, Ce, Pr, Nd, Sm, Eu, and Y (HREE were below detection limits in plagioclase).

cient evidence to claim that Henry's law constants are different at doped vs. natural concentration levels. He suggested that previously reported results (e.g., Harrison and Wood, 1980; Mysen, 1978) on the concentration dependence of reported D_ι's are likely to be analytical artifacts of the β-track autoradiography technique used in those studies. However, a variety of other techniques used to measure trace elements at low concentrations suggest that point and dislocational, equilibrium or nonequilibrium defects do exist at ~0.1–10 ppm level of trace element concentration (see Navrotsky, 1978; Urusov and Dudnikova, 1998). These defects may participate in exchange reactions with trace elements, increasing the value of partition coefficients at ppm levels of concentration. Defect sites can also be produced up to levels of several mole % as a result of trace element heterovalent substitutions, for example, as a result of REE-doping of feldspars (e.g., Kimata, 1988; D'Arco and Piriou, 1989; Kneip and Liebau, 1994).

It is not clear how experimental results with synthetic materials apply to complex natural systems in which minerals may contain tens to hundreds of ppm of total REE and thousands of ppm of all trace elements combined. Geochemical evidence, such as the constancy of Zr/Hf and Rb/K ratios in rocks (e.g., Watson, 1985), and the absence of odd–even anomalies in chondrite–normalized REE patterns, suggest that Henry's law is largely obeyed in fractionation processes in nature, even if it is not obeyed for some elements in certain experiments.

The ion microprobe is a reliable microbeam technique used to measure trace elements at sub-ppm levels of concentration, in the domain of potential failure of Henry's law. The experimental run products from the Drake (1972) plagioclase/natural basalt partitioning study provide an excellent set of samples to address these issues. In order to determine partition coefficients with the electron microprobe, Drake (1972) conducted many equivalent runs (with the same temperature and same plagioclase and melt compositions) doped with a variety of elements (Sr, Ba, or 1 to 4 selected REE). A few blank runs were also conducted with no doping. Since each of these equivalent runs was doped with one or few elements, it is possible to directly compare partition coefficients of all ion microprobe measurable elements depending *only* on the doping element. For example, partition coefficients for Sr can be studied in Sr-doped, Ba-doped, and REE- and Y-doped run series and in undoped run series. Such an approach allows us to consider not only the partitioning of different trace elements at doped vs. undoped levels (e.g., Bindeman et al., 1998), but also to check the dopant influence on partition coefficients of *undoped* elements.

We report here new ion microprobe analyses of the REE-doped and undoped plagioclase–basalt run products of Drake (1972). We made ion microprobe analyses for concentrations of a variety of undoped elements in three undoped runs (see Table 1). We also analyzed three more REE- and Y-doped samples, in addition to those reported in Bindeman et al. (1998). In combination with our analyses of Sr-doped runs, these new data allow us to compare D_ι's of trace elements in doped, Sr doped or undoped in *equivalent* runs.

2. ANALYTICAL TECHNIQUES

Analytical details are given in our first paper (Bindeman et al., 1998), and descriptions of experimental conditions are given in Drake (1972) and in Drake and Weill (1975). Table 1 summarizes conditions for their runs that were analyzed in this study.

Run products were first studied under reflected light and then with secondary and backscattered electron imaging on a JEOL JSM-5800LV scanning electron microscope. Electron microprobe analyses for major elements were made on a Cameca SX-50 electron microprobe using an accelerating voltage of 15 kV and a defocused beam of 10–25 nA (~2 μm) to minimize sodium loss. Two-μm step profiling was performed along and across several crystals within selected runs. We found that crystals are homogeneous within error with respect to mole % An and the major elements K, Fe, Mg, and Ti. Cathodoluminescence imaging of plagioclase in REE-doped, Sr-doped, and undoped runs also showed homogeneity within and among crystals in each run product analyzed. Given the ~10 μm ion microprobe beam diameter, we could only analyze (and report here) experimental products of in which the crystal size exceeded 15–20 μm, where it was possible to avoid overlap onto adjacent glass during the ion microprobe sputtering.

Ion microprobe analyses were made using the modified AEI IM-20 instrument at the University of Chicago (e.g., Hinton et al., 1988; Simon et al., 1994; MacPherson and Davis, 1994; Bindeman et al.,

1998). Calcium-normalized ion yields were obtained from a variety of natural and synthetic silicate standards. Previous experience (Hinton et al., 1988; MacPherson and Davis, 1994) has shown that there is little variation of ion yields in different silicate matrices under the energy-filtering conditions used in this work.

Since D_ι's of HREE heavier than Eu are normally below 0.01, HREE concentrations in typical igneous plagioclase and undoped experimental products are at the 10–100 ppb level. In addition, heavy REE have isobaric mass interferences from oxides of lighter REE and Ba (such as BaO on Eu and NdO and SmO on Dy). These effects are especially severe in high LREE/HREE phases such as plagioclase, so HREE were determined only at doped (80–200 ppm in plagioclase) concentration levels. Y, however, has a higher cosmic abundance than the HREE and no significant interferences and can be determined with reasonable precision even at the sub-ppm concentrations typical of natural plagioclases. Since Y has the same radius and valence as Dy and Ho (Shannon, 1976), it was used as a proxy for HREE.

3. RESULTS

3.1. Partition Coefficients of HREE and U

We have reanalyzed experimental run charges doped with HREE in order to accurately determine D_ι's for these elements, since the HREE were near electron microprobe detection limits in the earlier Drake and Weill (1975) study (Tables 2–4). In our electron microprobe reanalyzes (Bindeman et al., 1998), detection limits are 50–100 ppm; Drake and Weill did not give detection limits. Together with reanalyzed LREE-doped runs, the new analyses provide a consistent set of partitioning data for most of the REE at doped concentration levels for a range of plagioclase compositions. The partition coefficients for Gd, Dy, Er, and Lu and the linear regression of $\ln(D_{\mathrm{HREE}})$ vs. %An are presented on Figure 1 and are compared with the earlier Drake and Weill (1975) measurements and with existing volcanic phenocrysts/matrix determinations. We find that D_{Gd} is similar to the Drake and Weill (1975) value, while D_{Dy} and especially D_{Er} and D_{Lu} are increasingly discordant and the character of their %An dependence is different.

Concentrations of U in plagioclase are near detection limits in most runs but we find that our determinations of D_{U} are within the range of natural plagioclases from volcanic rocks (see Fig. 1) and observe that $\ln(D_{\mathrm{U}})$ has a strong dependence on %An, as is the case with other cations with high charge and large ionic radii (e.g., Bindeman et al., 1998).

We calculated the slopes and intercepts of the RT $\ln(D_\iota)$ vs. %An relationship using Williamson's (1968) regression routine which weights each analysis according to its uncertainty, and yields uncertainties in the slope and intercept:

$$\mathrm{RT}\ln(D_{\mathrm{U}}) = -484 \pm 195\%\mathrm{An} - 7452 \pm 12{,}552,$$

$$\mathrm{RT}\ln(D_{\mathrm{Dy}}) = -147 \pm 27\%\mathrm{An} - 35{,}075 \pm 1925,$$

$$\mathrm{RT}\ln(D_{\mathrm{Y}}) = -32 \pm 8\%\mathrm{An} - 59{,}700 \pm 592,$$

$$\mathrm{RT}\ln(D_{\mathrm{Gd}}) = -94 \pm 29\%\mathrm{An} - 30{,}234 \pm 1834,$$

$$\mathrm{RT}\ln(D_{\mathrm{Er}}) = -164 \pm 28\%\mathrm{An} - 40{,}087 \pm 1992,$$

and

$$\mathrm{RT}\ln(D_{\mathrm{Lu}}) = -80 \pm 7\%\mathrm{An} - 3318 \pm 515.$$

The linear fit is thermodynamically justified (e.g., Blundy and Wood, 1991) and the empirical dependence of $\ln D_\iota$ on %An is of good practical value for choosing a D_ι for measured %An in a natural plagioclase. These approximation parameters for Dy, Y, Gd, Er, Lu at doped concentration levels supersede those reported in our earlier study (Bindeman et al., 1998) and are recommended for use.

3.2. $\ln(D_\iota)$ vs. %An and RT $\ln(D_\iota)$ vs. %An Dependencies as a Function of Trace Element Size and Charge

A comparison of the slopes of the $\ln(D_\iota)$ dependencies on %An for the REE shows a regular decrease of slope from strongly negative (La) to weakly positive (Lu) (Fig. 2a). Bindeman et al. (1998) observed a similar effect for plagioclase/melt partition coefficients for monovalent and divalent cations. Those cations that are similar, or smaller, in size than that of the *M*-site (e.g., Li and Mg) exhibit a positive slope in their $\ln(D_\iota)$ vs. %An dependence, while almost all other elements show negative slopes.

The REE are a group of trace elements that exhibit gradual decrease in atomic radii with increasing atomic number, and the observed smooth changes in partitioning behavior are to be expected. In order to explain the fan-like trend shown in Figure 2a, we used the thermodynamic elastic modulus approach of Brice (1975) elaborated by Blundy and Wood (1994) for partitioning studies. In this model, at each temperature and pressure, partition coefficients of trace elements of each valence group can be described as a function of three parameters: the optimum radius of the lattice site in plagioclase structure, r_0; the "strain-compensated" partition coefficients, D_0, for strain free substitution; and the Young's modulus, E, of plagioclase. The elastic modulus model describes a near parabola when calculated partition coefficients are plotted on a $\ln(D_\iota)$ vs. ionic radius graph. Experimentally and naturally determined partition coefficients of trace elements lie along inverted parabolas on $\ln(D_\iota)$ vs. ionic radius plots when grouped by valence (e.g., Onuma et al., 1968).

Application of the model to our data yielded a similarly fan-like trend between LREE and HREE with decreasing An (Fig. 2b). The difference in the slopes of the $\ln(D_\iota)$ vs. %An dependence for LREE vs. HREE leads to partition coefficient ratios, such as $D_{\mathrm{La}}/D_{\mathrm{Lu}}$ and $D_{\mathrm{La}}/D_{\mathrm{Y}}$, that are very sensitive to plagioclase composition (Fig. 3): anorthite exhibits the smallest $D_{\mathrm{La}}/D_{\mathrm{Y}}$ and $D_{\mathrm{La/Y}}$ ratios and albite the largest ones. This suggests that plagioclase of variable composition is capable of changing the geochemically indicative LREE/HREE ratios by up to one order of magnitude for a reasonable An range (e.g., An_{80} to An_{40}) within a single zoned grain of plagioclase. The reconstruction of parent melt REE patterns assuming constant partition coefficients ratios, therefore, can be quite misleading.

The RT $\ln(D_\iota)$ vs. %An dependence resembles the $\ln(D_\iota)$ vs. %An dependence, since the temperature difference between high and low temperature experiments is only 144°C and is in the high temperature interval where temperature differences have smaller effects (see Table 1). This translates to a less than 10% variation in RT $\ln(D_\iota)$ parameters as compared to those for $\ln(D_\iota)$. The slopes of the RT $\ln(D_\iota)$ vs. %An dependencies increase with increasing ionic radius for REE and monovalent and divalent cations entering the *M* site (Bindeman et al., 1998) (Fig. 4). For divalent cations (Mg, Ca, Sr, and Ba) there is an

Table 2. Plagioclase compositions from REE-doped and undoped runs. Oxide concentrations are given in wt.% and element compositions are given in ppm. The dopant concentrations are underlined. Uncertainties are based on the greater of counting statistics or replicate analyses and are only given when they exceed 5% of the amount present. Upper limits are $<2\sigma$.

	99-1	100-1	101-1	94-7	99-7	99-2	99-5	100-4	100-6	101-4	101-3	101-7
# anal.	4	3	3	13	2	3	2	3	3	2	2	2
An%	51.5 ± 0.8	66.2 ± 0.9	71.3 ± 0.6	39.8 ± 0.5	50.7 ± 0.2	50.6 ± 0.7	49.1 ± 1.5	53.9 ± 0.5	66.3 ± 0.5	69.9 ± 0.3	71.8 ± 2.1	70.1 ± 0.7
Na_2O	5.50	3.37	2.90	6.51	5.51	5.38	6.13	3.97	3.50	3.00	3.13	3.19
Al_2O_3	29.7	32.3	33.2	25.2	29.3	29.1	29.1	31.9	32.1	32.3	33.2	32.8
SiO_2	50.5	47.7	46.2	57.4	51.4	52.1	50.1	46.7	47.8	48.2	44.8	46.3
CaO	12.3	14.8	16.2	8.56	11.8	11.4	12.3	15.3	14.9	15.0	17.1	16.2
FeO	1.43	1.29	1.09	1.00	1.25	1.18	1.41	1.22	1.05	0.81	0.91	0.93
ΣLn_2O_3	0.00	0.00	0.00	0.77	0.14	0.28	0.02	0.32	0.09	0.03	0.40	0.10
Li	11.5	22.5 ± 1.8	31.4	4.38	11.9 ± 0.6	14.1	24.2	30.9	50.1	11.6	21.3	10.5
Be	1.60 ± 0.33	1.38 ± 0.18	1.21 ± 0.30	0.124 ± 0.035	1.22 ± 0.20	1.37 ± 0.09	0.683 ± 0.044	0.79 ± 0.24	0.463 ± 0.088	0.452 ± 0.067	1.52	1.47
B	3.43 ± 0.67	1.46 ± 0.56	3.33 ± 0.39	1.35 ± 0.25	4.94	9.2 ± 2.8	7.12 ± 0.60	6.69 ± 0.62	4.26 ± 0.90	25 ± 17	2.25 ± 0.29	6.59 ± 0.73
Mg	1017	1047	1036 ± 58	773 ± 51	1013 ± 215	834	979 ± 124	1032 ± 160	938	760	828	838
P	95 ± 15	76 ± 35	45 ± 16	126 ± 16	82 ± 16	90 ± 14	71 ± 17	56 ± 18	43 ± 29	52 ± 15	35.7 ± 6.3	67 ± 11
K	1206	1015 ± 73	1011	1007	1294	1359	1611 ± 127	1482 ± 216	1163	1060	929 ± 104	1228 ± 78
Ti	513 ± 26	368 ± 20	433 ± 31	424	491 ± 34	415 ± 31	463	384 ± 58	379	323 ± 35	260 ± 21	335
Rb	0.82 ± 0.43	<0.67	0.80 ± 0.29	0.95 ± 0.23	0.95 ± 0.48	0.69 ± 0.34	1.00 ± 0.42	0.81 ± 0.67	<0.64	<0.48	1.34 ± 0.73	0.99 ± 0.34
Sr	1076	804	626	986	1096	1098	1111	912 ± 71	804	550	614 ± 35	647
Y	0.431 ± 0.043	0.655 ± 0.063	0.52 ± 0.12	0.91 ± 0.11	1.00 ± 0.28	0.489 ± 0.079	140 ± 9	186 ± 42	0.66 ± 0.14	126 ± 7	0.751 ± 0.079	0.589 ± 0.077
Zr	0.45 ± 0.22	0.35 ± 0.10	0.49 ± 0.19	0.77 ± 0.18	0.227 ± 0.083	0.40 ± 0.14	0.58 ± 0.28	1.50 ± 0.78	0.262 ± 0.094	0.334 ± 0.086	0.374 ± 0.066	0.41 ± 0.12
Ba	128 ± 8	82.1	84 ± 14	207	147	185	147	95.5 ± 7.8	81.8	59.1	75 ± 16	71 ± 12
La	2.11 ± 0.15	1.64 ± 0.15	1.70 ± 0.19	6572	3.58	2.20 ± 0.28	2192 ± 119	1135 ± 63	1.89 ± 0.11	1079	1.61 ± 0.16	1.93 ± 0.24
Ce	3.17 ± 0.19	2.75 ± 0.30	2.72 ± 0.49	11.9 ± 0.9	6.40	2.83 ± 0.21	687 ± 41	1443 ± 95	3.32 ± 0.23	1110	2.36 ± 0.25	2.78 ± 0.21
Pr	0.360 ± 0.046	0.373 ± 0.046	0.365 ± 0.039	1.16 ± 0.12	0.68 ± 0.20	0.47 ± 0.11	0.43 ± 0.11	0.42 ± 0.15	0.33 ± 0.09	0.23 ± 0.1	0.475 ± 0.062	0.470 ± 0.092
Nd	1.14 ± 0.11	1.39 ± 0.13	1.40 ± 0.14	4.20 ± 0.34	593	12.1 ± 6.1	1.74 ± 0.68	1.21 ± 0.32	303	0.79 ± 0.37	5.2 ± 3.3	661 ± 51
Sm	0.458 ± 0.083	0.509 ± 0.091	0.42 ± 0.12	0.586 ± 0.073	<0.79	1268	0.62 ± 0.16	0.39 ± 0.29	<0.79	0.59 ± 0.11	1686	0.39 ± 0.21
Eu	0.104 ± 0.064	0.173 ± 0.055	0.123 ± 0.078	0.72 ± 0.15	0.31 ± 0.14	637	0.54 ± 0.10	1.45 ± 0.41	0.11 ± 0.10	0.874 ± 0.067	984	<0.33
Gd						463					769	
Dy					336				267			137
Er					279				159			84.2 ± 5.9
Lu							34.4	135 ± 30		128 ± 9		
U					0.103 ± 0.038	0.151 ± 0.084	0.061 ± 0.030	0.077 ± 0.030	0.072 ± 0.030	<0.058	<0.044	0.042 ± 0.021

Table 3. Glass compositions from REE-doped and undoped runs. Oxide concentrations are given in wt.% and element compositions are given in ppm. The dopant concentrations are underlined. Uncertainties are based on the greater of counting statistics or replicate analyses and are only given when they exceed 5% of the amount present. Upper limits are $<2\sigma$.

	99-1	100-1	101-1	94-7	99-7	99-2	99-5	100-4	100-6	101-4	101-3	101-7
# anal.	3	3	3	2	2	2	2	4	2	2	2	2
Na_2O	5.61	3.63	3.23	7.32	5.61	5.44	6.87	4.46	3.84	3.80	4.15	3.89
Al_2O_3	15.7	17.0	18.8	15.2	17.2	17.1	17.6	18.0	17.5	20.6	20.8	20.5
SiO_2	62.5	60.8	58.0	62.5	57.5	56.3	55.1	54.1	58.4	50.6	47.5	53.2
CaO	4.65	6.76	8.34	3.63	4.92	5.11	5.41	7.74	7.22	9.21	9.86	9.21
FeO	5.13	5.59	5.35	3.65	4.93	5.26	5.46	5.31	4.72	5.17	5.06	5.00
ΣLn_2O_3	0.01	0.01	0.01	2.86	3.59	4.66	1.26	3.61	2.20	2.22	6.71	1.92
Li	36.2	74.0	106	17.9 ± 1.2	44.0	52.6 ± 3.4	95.2	107	185 ± 10	46.8	94.4	41.6
Be	1.81 ± 0.11	1.33 ± 0.13	1.45 ± 0.14	0.431 ± 0.040	2.08 ± 0.24	2.08	1.83 ± 0.13	1.02	1.01 ± 0.08	0.955 ± 0.050	1.47 ± 0.14	1.87 ± 0.20
B	28.2 ± 1.6	22.8 ± 1.5	22.2	6.78 ± 0.40	21.8 ± 1.5	43.1 ± 2.8	51.0	25.0 ± 2.2	24.5 ± 1.4	37.1 ± 5.2	15.9	28.7
Mg	24212	23516	24225	17402 ± 1185	22109	23309	22378	21744	21940	22143	22204	23579
P	924	623 ± 45	545 ± 33	1184 ± 74	940	872	880	474 ± 41	610 ± 87	556	342 ± 19	463
K	7845	7547	7161	5786	7680	7043	10338	8998	8158	8839	7926	8469
Ti	5761	5662	5551	4411	5508	5587	5777	5437	5404	5650	5394	5488
Rb	26.3	20.0	19.3 ± 1.4	28.7 ± 1.7	56.9	29.0	36.8 ± 2.1	23.1	38.3 ± 4.2	20.8 ± 1.1	22.7	31.2
Sr	340	384	329	295 ± 33	391	386	423	452 ± 25	400	366	380	385
Y	14.9	15.5	16.6	14.2 ± 1.2	26.9	20.0 ± 2.1	5910	6229	24.0	5570	24.2	23.7
Zr	102	112	119	81.0	106	102	107	103	107	123	105	114 ± 9
Ba	330	296	306	312	341	367	364	368 ± 25	301	323	372	335
La	8.24	8.03 ± 0.47	9.20	24337 ± 2990	13.2 ± 0.7	9.58	9944	6481	9.74 ± 0.74	7675	10.4	11.8 ± 0.6
Ce	20.0	20.5	22.4	25.3 ± 1.4	38.4	21.1	5015	12680	28.3	11680	24.5	29.3
Pr	2.47	2.48 ± 0.19	2.62 ± 0.18	2.82	4.88 ± 0.47	3.27 ± 0.26	3.45 ± 0.22	4.60 ± 0.33	2.80 ± 0.27	3.57 ± 0.41	3.60	4.07 ± 0.27
Nd	9.26	10.5	11.5	10.9 ± 0.6	4846	<82	10.3 ± 0.6	11.7 ± 1.1	2895	10.7 ± 0.93	152 ± 16	7281
Sm	4.69	3.55 ± 0.18	3.00 ± 0.16	2.69	6.18 ± 0.71	20279	5.83	9.8 ± 2.0	4.3 ± 1.6	7.67 ± 0.53	26798	3.30 ± 0.74
Eu	0.71 ± 0.10	1.04 ± 0.12	1.41 ± 0.11	<0.19	2.55 ± 0.28	9508	7.37	16.2 ± 1.1	2.13 ± 0.26	14.0	14260	2.62 ± 0.25
Gd						10023 ± 508					15314	
Dy					11197				8415			4662
Er					15111				7731			4657
Lu							4997	11877		13785		
U					2.62 ± 0.19	2.06 ± 0.15	1.54 ± 0.11	1.01 ± 0.08	1.37 ± 0.25	0.91 ± 0.16	0.868 ± 0.064	3.92 ± 0.28

Table 4. Plagioclase/melt partition coefficients from REE-doped and undoped runs. The dopant partition coefficients are underlined. Uncertainties are propagated from uncertainties of concentrations in plagioclase and glass and are only given when they exceed 5% of the amount. Upper limits are $<2\sigma$.

	99-1	100-1	101-1	94-7	99-7	99-2	99-5	100-4	100-6	101-4	101-3	101-7
Li	0.317	0.305 ± 0.024	0.296	0.245 ± 0.018	0.272 ± 0.019	0.268 ± 0.020	0.254	0.288	0.271 ± 0.014	0.247	0.225	0.252
Be	0.88 ± 0.19	1.04 ± 0.17	0.84 ± 0.22	0.288 ± 0.085	0.58 ± 0.12	0.656 ± 0.048	0.373 ± 0.035	0.77 ± 0.24	0.457 ± 0.094	0.473 ± 0.074	1.03 ± 0.10	0.787 ± 0.089
B	0.122 ± 0.025	0.064 ± 0.025	0.150 ± 0.019	0.199 ± 0.038	0.226 ± 0.019	0.213 ± 0.066	0.139 ± 0.012	0.267 ± 0.034	0.174 ± 0.038	0.69 ± 0.48	0.142 ± 0.019	0.230 ± 0.026
Na	0.981	0.930	0.897	0.889	0.983	0.989	0.893	0.889 ± 0.048	0.914	0.789	0.754 ± 0.067	0.820
Mg	0.0420	0.0445	0.0427 ± 0.0025	0.0444 ± 0.0042	0.046 ± 0.010	0.0358	0.0437 ± 0.0057	0.0474 ± 0.0074	0.0428	0.0343	0.0373	0.0355
Al	1.90	1.90	1.76	1.66	1.70	1.71	1.65	1.78	1.83	1.57	1.59	1.60
Si	0.808	0.785	0.796	0.919	0.895	0.925	0.910	0.863	0.819	0.954	0.944	0.871
P	0.103 ± 0.017	0.123 ± 0.057	0.082 ± 0.031	0.106 ± 0.015	0.087 ± 0.017	0.103 ± 0.017	0.081 ± 0.019	0.118 ± 0.039	0.071 ± 0.048	0.094 ± 0.028	0.104 ± 0.019	0.145 ± 0.024
K	0.154	0.135 ± 0.010	0.141	0.174 ± 0.009	0.168	0.193	0.156 ± 0.013	0.165 ± 0.025	0.143	0.120	0.117 ± 0.013	0.145 ± 0.009
Ca	2.68	2.19	1.94	2.36 ± 0.19	2.39	2.23	2.26 ± 0.11	1.98	2.07	1.62	1.74	1.76
Ti	0.0891 ± 0.0046	0.0650 ± 0.0037	0.0780 ± 0.0056	0.0962 ± 0.0055	0.0892 ± 0.0064	0.0743 ± 0.0057	0.0801	0.071 ± 0.011	0.0701	0.0572 ± 0.0062	0.0482 ± 0.0039	0.0611
Fe	0.279	0.230	0.204	0.275	0.253	0.224 ± 0.022	0.258	0.229 ± 0.021	0.222 ± 0.012	0.157	0.181	0.185 ± 0.010
Rb	0.031 ± 0.016	<0.033	0.042 ± 0.015	0.0331 ± 0.0082	0.0166 ± 0.0084	0.024 ± 0.012	0.027 ± 0.011	0.035 ± 0.029	<0.017	<0.023	0.059 ± 0.032	0.032 ± 0.011
Sr	3.17	2.10	1.90	3.34 ± 0.39	2.80	2.84	2.63	2.02 ± 0.19	2.01	1.50	1.61 ± 0.09	1.68
Y	0.0289 ± 0.0029	0.0423 ± 0.0044	0.0315 ± 0.0072	0.0641 ± 0.0092	0.037 ± 0.010	0.0244 ± 0.0047	0.0238 ± 0.0017	0.0298 ± 0.0067	0.0274 ± 0.0059	0.0227 ± 0.0013	0.0311 ± 0.0033	0.0248 ± 0.0033
Zr	0.0044 ± 0.0021	0.00308 ± 0.00091	0.0042 ± 0.0016	0.0096 ± 0.0022	0.00215 ± 0.00078	0.0039 ± 0.0014	0.0054 ± 0.0027	0.0146 ± 0.0076	0.00245 ± 0.00088	0.00272 ± 0.00071	0.00355 ± 0.00063	0.0037 ± 0.0011
Ba	0.389 ± 0.024	0.277	0.277 ± 0.048	0.661 ± 0.039	0.432 ± 0.023	0.504	0.403	0.259 ± 0.028	0.272	0.183	0.200 ± 0.044	0.211 ± 0.037
La	0.256 ± 0.020	0.205 ± 0.022	0.184 ± 0.021	0.270 ± 0.035	0.271 ± 0.019	0.229 ± 0.030	0.220 ± 0.013	0.175 ± 0.012	0.194 ± 0.018	0.141	0.155 ± 0.015	0.163 ± 0.022
Ce	0.159 ± 0.010	0.134 ± 0.015	0.121 ± 0.022	0.470 ± 0.043	0.167 ± 0.009	0.134 ± 0.011	0.137 ± 0.009	0.114 ± 0.009	0.117 ± 0.009	0.0950	0.096 ± 0.011	0.950 ± 0.0075
Pr	0.146 ± 0.020	0.150 ± 0.022	0.139 ± 0.018	0.412 ± 0.043	0.139 ± 0.043	0.142 ± 0.034	0.124 ± 0.032	0.091 ± 0.033	0.118 ± 0.034	0.063 ± 0.019	0.132 ± 0.018	0.116 ± 0.024
Nd	0.123 ± 0.012	0.133 ± 0.013	0.121 ± 0.013	0.386 ± 0.038	0.122 ± 0.004	<0.73	0.168 ± 0.066	0.104 ± 0.029	0.105	0.074 ± 0.036	0.034 ± 0.022	0.0908 ± 0.0071
Sm	0.098 ± 0.018	0.144 ± 0.027	0.139 ± 0.041	0.218 ± 0.029	<0.13	0.0625	0.106 ± 0.028	0.040 ± 0.031	<0.19	0.077 ± 0.016	0.0629	0.117 ± 0.068
Eu	0.148 ± 0.093	0.166 ± 0.056	0.088 ± 0.056	<0.64	0.123 ± 0.056	0.0670	0.073 ± 0.014	0.089 ± 0.026	0.053 ± 0.045	0.0623 ± 0.0049	0.0690	<0.13
Gd						0.0461 ± 0.0032					0.0502	
Dy					0.0300				0.0318			0.0293
Er					0.0185				0.0206			0.0181 ± 0.0013
Lu							0.00687	0.0114 ± 0.0025		0.00927 ± 0.00069		
U					0.039 ± 0.015	0.073 ± 0.041	0.039 ± 0.020	0.076 ± 0.030	0.053 ± 0.024	<0.065	<0.051	0.0107 ± 0.0054

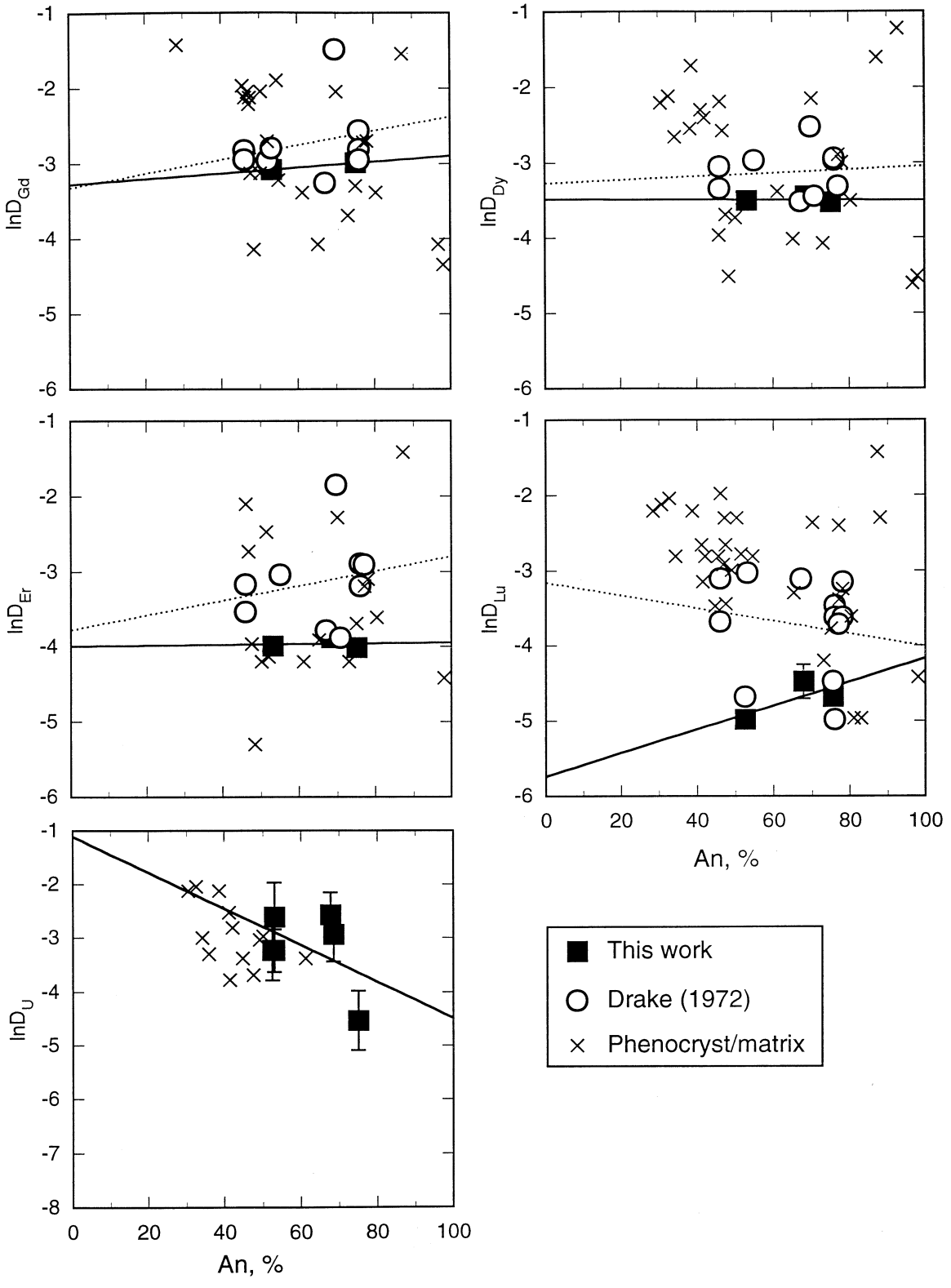

Fig. 1. Partition coefficients of HREE and U as a function of %An. The solid lines are linear regressions through our ion microprobe-measured partition coefficients; dashed lines are linear regressions through Drake's (1972) electron microprobe-measured partition coefficients. U is at its natural concentration level, HREE are at doped concentrations. Phenocryst/matrix partition coefficients are taken from: Nagasawa and Schnetzler (1971); Schnetzler and Philpotts (1970); Vernieres et al., 1977; Nash and Crecraft, 1985; Higuchi and Nagasawa, 1969; Dudais et al., 1971; Dunn and Sen, 1994; Fujimaki et al., 1984; Francalanci (1989); Phinney, 1992; Worner et al., (1983).

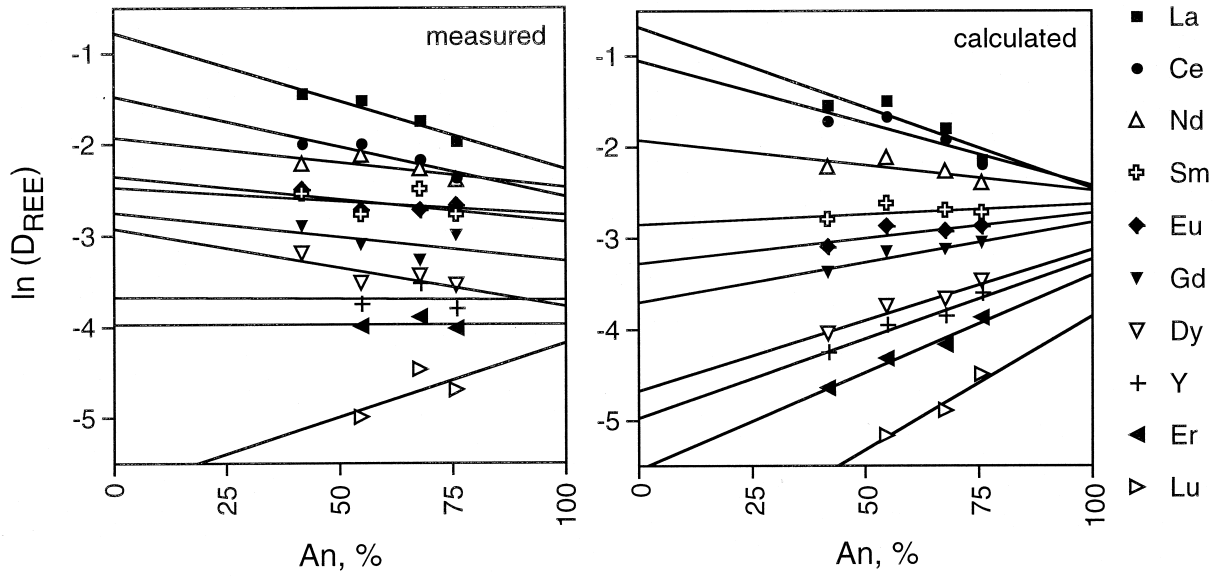

Fig. 2. (a) The slope of the $\ln(D_{REE})$ vs. %An dependence decreases with decreasing REE atomic number (increasing ionic radius) from Lu to La. Measured D_{REE} from experiments doped with those REE are from this study (see Fig. 1) and Bindeman et al. (1998). (b) Calculated slopes using the Blundy and Wood (1994) elastic modulus model based on the *measured* D_i of one middle REE, Nd. Formula (3) of Blundy and Wood (1994) was used to predict the values of D_{REE}. This approach allowed us to avoid offsets and is best for comparing of D_i's of neighboring REE (cf. Wood and Blundy, 1997). The size of the *M* site for strain-free substitution of REE^{3+} (r_0) for the four studied plagioclase compositions was taken from the maxima of the REE parabolas on Onuma diagrams (cf. Fig. 5) and are 1.224 Å for An_{45}, 1.215 Å for An_{55}, 1.200 Å for An_{65} and 1.172 Å for An_{75}. A linear fit to these values yielded $r_0 = 1.29$ for albite and 1.15 for anorthite, which is within the range determined from bulk elastic properties of plagioclase (Angel et al., 1988) and the Blundy and Wood (1994) partitioning data. We used *E* and r_0 values (in kbars) (2084) for albite and (1903) anorthite from Blundy and Wood (1994) and assumed that *E* is a linear function of %An in order to obtain *E* values for our plagioclases of intermediate composition. Discrepancies for larger and smaller REE may result from the assumed linear relationship of *E* and r_0 with %An and/or partial partitioning of smaller ions (e.g., Mg) into the *T* site (e.g., Peters et al., 1995).

excellent overall agreement between observed D_i's and those calculated with the Blundy and Wood (1994) model and the slopes of $\ln(D_i)$ and RT $\ln(D_i)$ vs. %An dependence (except for Mg, which shows a slope of opposite sign). For monovalent cations (Li, Na, K, Rb) there is a good agreement with the Blundy and Wood (1994) model, with larger discrepancies for smallest cation, lithium, for which the model predicts lower D_i slightly beyond our analytical uncertainty for both values and slopes.

Both our measurements and the Blundy and Wood (1994) model give an increase of RT $\ln(D_i)$ vs. %An slope with increasing ionic radius and increasing cation charge, and the magnitude of slope variation within each valence group increases from monovalent to trivalent cations. These effects can be understood by consideration of an Onuma diagram [$\ln(D_i)$ vs. ionic radius) (Onuma et al., 1968). The thermodynamic significance of Onuma diagrams can be explained using the relation discovered by Brice (1975) on the dependence of the free energy of the exchange of a trace element between crystal and melt with the magnitude of its strain of the crystal lattice. In Figure 5, parabolic curves, based on Eqn. 2 of Blundy and Wood (1994), are fitted through partition coefficients of most anorthite-rich (thick lines) and anorthite-poor (thin line) of analyzed runs (Bindeman et al., 1998). These curves show that with an increase in albite content the parabola maximum (indicating the size of *M*-site) shifts to the right, because the size of the *M*-site in albite is larger than that in anorthite in accor-

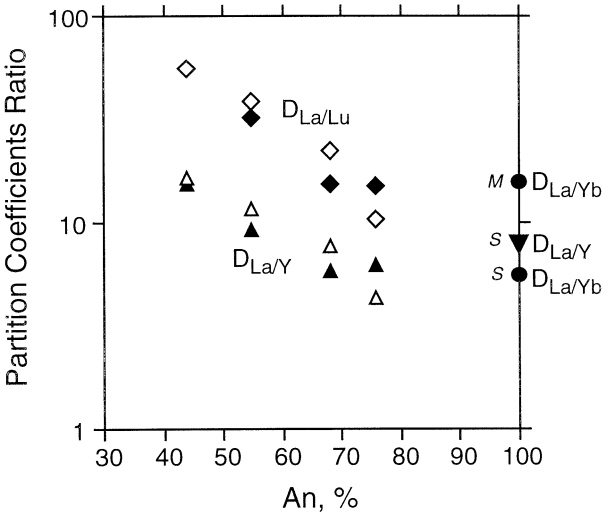

Fig. 3. $D_{La/Lu}$ and $D_{La/Y}$ increase with decreasing An content of plagioclase. Filled symbols are ion microprobe-measured values, open symbols are calculated values based on the Blundy and Wood (1994) model (see Fig. 2 for description). Note that both measured and calculated $D_{La/Lu}$ and $D_{La/Y}$ yield a similar increase with decreasing An%. $D_{La/Yb}$ and $D_{La/Y}$ values based on anorthite-CAI melt experiments of Simon et al. (1994) and McKay et al. (1994) are shown for comparison.

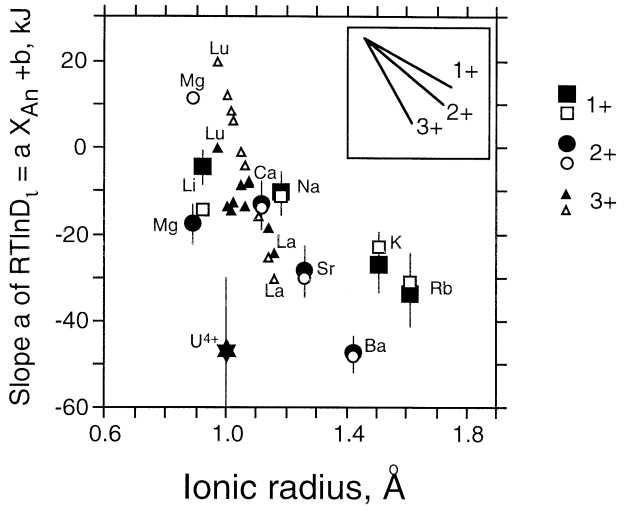

Fig. 4. Comparison of measured (filled symbols) and calculated [using the Blundy and Wood (1994) approach, open symbols] slopes of the RT $\ln(D_\iota) = a\,X_{An} + b$ dependence for monovalent, divalent and trivalent cations as a function of their ionic radii at eightfold coordination (from Shannon, 1976). Note that the dependence becomes steeper with increasing valence number, meaning that D_ι of higher charged ions are more sensitive to the anorthite content of plagioclase.

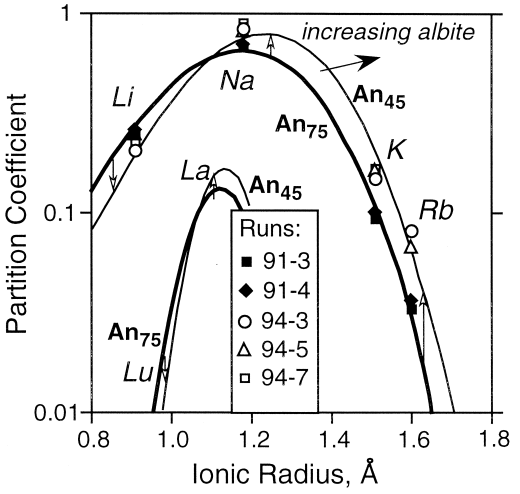

Fig. 5. An Onuma diagram, with near parabolic curves fitted through partition coefficients of the most anorthite-rich (thick lines) and anorthite-poor (thin line) of the analyzed runs (Bindeman et al., 1998). The top of each parabola indicate the size of the site (M site), r_0, and the partition coefficients, D_0, of the strain free substitution (e.g., Onuma et al., 1968). Equation 2 from Blundy and Wood (1994) was used for nonlinear fitting with three free parameters: r_0, D_0 and the Young moduli, E. Notice that the parabolas shift to the right and up, indicating the increase in r_0 and D_0 with decreasing %An. Vertical arrows show the magnitude of D_ι increase for trace elements at each ionic radius. D_ι of ions whose radius is closer to r_0 (e.g., Na) do not show a large increase in D_ι; the larger ions Rb and La show a significant increase in D_ι, while the smaller ions Li and Lu show a decrease in D_ι with decreasing %An. This explains the $\ln D_\iota$ vs %An seen in Figs. 2–4 and Bindeman et al. (1998).

dance with larger Na–O than Ca–O interatomic distance (Angel et al., 1988). Partition coefficients of ions whose radius is closer to the parabola maximum (e.g., Na, middle REE) do not show a large increase; D_ι of larger ions (e.g., Rb and La) show a significant increase, while D_ι of smaller ions (e.g., Li and Lu) show a decrease.

The dependence of the slope on ionic charge is also explained by consideration of Figure 5. Since the parabola fitted through the trivalent REE group is narrower than the parabola for monovalent group, an equivalent shift of parabola maxima to the right (larger ionic radius) produces a larger relative effect of slope change per unit of ionic radius increase for trivalent than monovalent ions, explaining the behavior shown in Figure 4.

To summarize, we observe a general tendency of increasing slope of the $\ln(D_\iota)$ vs. %An and RT $\ln(D_\iota)$ vs. %An dependencies with increasing ionic *size* and *charge*. REE group and higher-charged ions are the most sensitive to plagioclase composition change, while alkalis are least sensitive. This has an important general implication: partition coefficients of the larger and higher valence ions of each valence group and their ratios (e.g., Fig. 3) may vary significantly with %An.

3.3. REE Spectrum Partitioning at Doped Concentrations

We find that for four studied plagioclase compositions, $\ln(D_{REE})$ decreases linearly with increasing atomic number (Fig. 6). We also observe that $\ln(D_{REE})$ exhibit steeper slope for more albitic plagioclase, in accordance with increasingly divergent D_{LREE} vs. D_{HREE} in Figure 2. Since Drake's experiments were conducted in air, Eu is almost entirely trivalent (e.g., Drake, 1975; Wilke and Behrens, 1999), and behaves like the rest of the REE. However, a very small Eu positive peak is still discernible and is likely to be due to a small portion (~1%, Wilke and Behrens, 1999) of total Eu that is present as Eu^{2+} and partitions 20 to 100 times more efficiently into plagioclase, causing $D_{Eu}^{(total)}$ be higher. On the contrary, the negative deviation of Ce from the straight line may be related to the fact that Ce is partly tetravalent, and is less favored by the plagioclase structure. Schreiber et al. (1980) found that Ce^{4+} can constitute up to 10–20% of total Ce in different basaltic systems in experiments conducted in air.

Using Blundy and Wood's (1994) model we are able to reproduce a linear drop in D_{REE} with REE atomic number for four plagioclase compositions (Fig. 6), which clearly demonstrates that REE at doped concentrations partition into the M site. We conclude that a linear drop in $\ln(D_{REE})$ with REE atomic number is likely to be a general pattern of plagioclase-melt partitioning, and is not an artifact of our measurements or a specific result of the Drake experiments. Significantly, we observe that the pattern of $\ln(D_{REE})$ becomes steeper with decreasing anorthite content in plagioclase (Figs. 6 and 3) for both measurements and calculations.

The existence of a linear $\ln(D_{REE})$ vs. ionic radius dependence is not an expected result. Most previous experiments and bulk phenocryst/matrix studies produced a progressively shallowing concave-up $\ln(D_{REE})$-atomic number pattern, and this partition behavior seems to be taken for granted by many users. However, such apparent partitioning behavior can be an artifact caused by two offsetting errors. It is likely that there was an overestimation of HREE in plagioclase (because of analytical

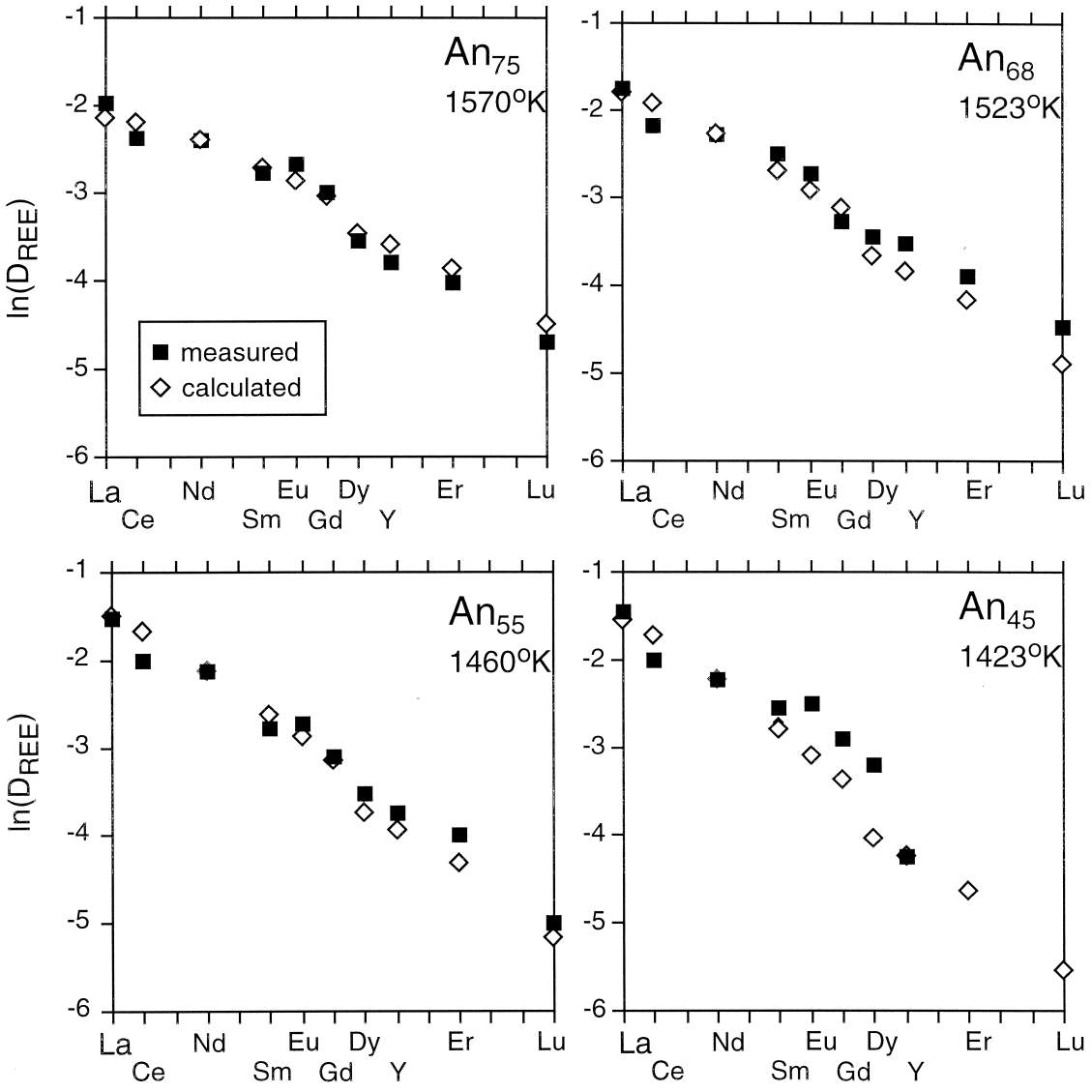

Fig. 6. Measured D_{REE} for REE-doped runs compared with D_{REE} calculated using the Blundy and Wood (1994) model; see Fig. 2 and text for discussion. Note the linear drop in D_{REE} in both calculated and measured results and the steepening of the slope with the decreasing An content of plagioclase.

interferences and concentrations near the detection limit) in earlier electron microprobe-based experimental partitioning studies, including Drake's. On the other hand, in phenocryst/matrix bulk determinations of partition coefficients, microinclusions of apatite, zircon and other accessory minerals as well as clinopyroxene and amphibole are often present in plagioclase and it is difficult to separate inclusions from plagioclase using conventional techniques. These minerals are strongly enriched in HREE relative to LREE (e.g., Watson and Harrison, 1984) and this may lead to overestimation of D_{HREE} in bulk measurements of natural plagioclases. However, some experimental and volcanic studies do show a straight line in $\ln(D_{REE})$-atomic number coordinates. McKay et al. (1994) and Simon et al. (1994) found similar patterns between anorthite and CAI-type melt in doped experiments analyzed by ion microprobe. Phenocryst/matrix partition coefficients by Phinney and Morrison (1990) derived from neutron activation analyses also plot as a straight line.

3.4. Difference Between D_{REE} in REE-Undoped and REE-Doped Samples

The analyzed D_{REE} for *undoped* REE at natural concentration levels determined on undoped and Sr-doped runs are plotted in Fig. 7 and compared with *doped* D_{REE} in REE-doped runs as a function of REE atomic number. We find that undoped REE in runs doped with Sr behave similar to REE in undoped runs (Fig. 7), signifying that there is no influence of variable concentrations of Sr on REE partitioning. For the three studied plagioclase compositions, D_i's of undoped REE are higher than that of doped REE. The difference in D_i's is not large for some LREE, but there is a tendency of $\ln(D_{REE})$ of

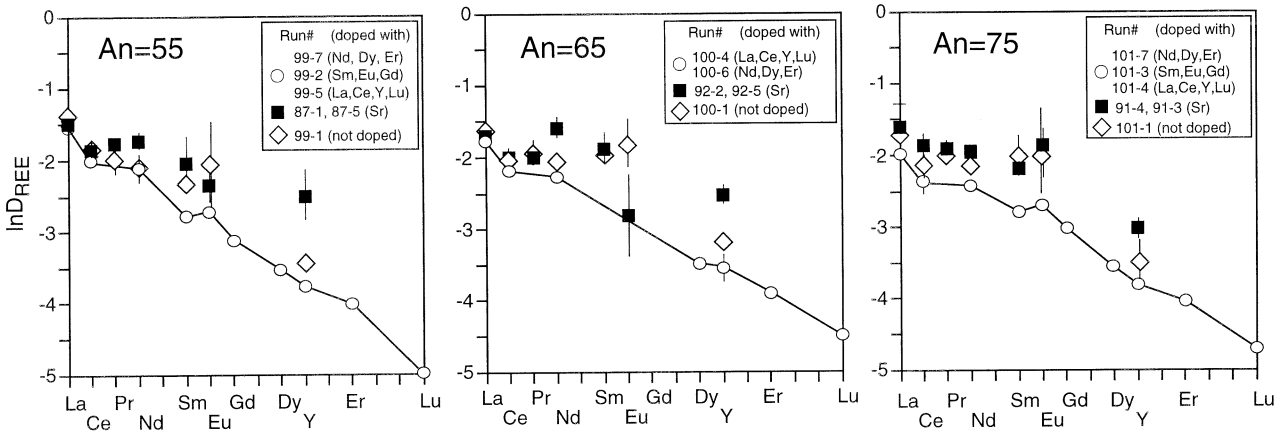

Fig. 7. REE and Y partition coefficients ($\pm 1\ \sigma$) at natural concentration levels of REE (~0.3–3 ppm) measured on Sr-doped runs and undoped runs compared with those measured at doped concentration level in REE and Y doped runs.

undoped REE be systematically higher for several studied plagioclase compositions for the whole spectrum of REE (Fig. 7). Therefore, the difference between otherwise equivalent runs (same temperature and major element composition, same ion microprobe analytical conditions, but different doping element) is significant. Averaged undoped D_{REE} are directly compared to REE-doped D_{REE} in these equivalent runs as a function of each REE concentration (Fig. 8a). The ~30 to 100% increase in D_{REE} with decreasing concentration (and its slope) are similar for different REE in each run, and in between different runs. The increase does not change D_{REE} relative to one another, and undoped D_{REE} obey the same Onuma diagram relationship as doped D_{REE} in equivalent runs (Bindeman et al., 1998). This regular and parallel fashion of D_{REE} increase with decreasing concentration suggests that REE are partitioned structurally at doped and natural concentration levels. (See Tables 2–4.)

Since Drake normally doped his runs with 3 to 4 selected REE, the D_ι's of other, *undoped* REE in these REE-doped runs is interesting to consider (Fig. 9). La–Ce–Y–Lu, Sm–Eu–Gd, and Nd–Dy–Er run series were conducted (see Table 1) for each plagioclase composition. For example, it is possible to compare D_{Sm} in the La–Ce–Y–Lu and Nd–Dy–Er doping series where Sm is at natural concentrations with D_{Sm} in the Sm–Eu–Gd series in which Sm was a doping element. The goal is to check if doping with selected REE changes D_{REE} of the whole spectrum (including undoped REE in REE-doped runs) or the undoped REE follows the same partition behavior as in REE-undoped runs. In particular, if an undoped REE (X) in a run doped with other REE gives a lower D_X for doped concentrations (as it would if the run were doped with rare earth element X), the REE spectrum will be smooth. If D_X turns out to be high, as it would in a run not doped with any REE, a positive anomaly would appear in the REE spectrum at that point. Figures 8b and 9 present D_{REE} for both doped and undoped REE in each run series for three plagioclase compositions. Despite the significant analytical uncertainty, we observe that D_{REE} values tend to follow the same pattern as for doped REE. We conclude that there is an influence of doping with REE on D_{REE} values for undoped REE. By comparing Figure 7 with Figure 9, or more clearly by comparing Figures 8a,b, it can be seen that doping with REE strongly subdues the effect of undoped D_{REE} increase with decreasing concentration.

3.5. Partition Coefficients of Trace Elements in Runs Doped with REE, Y, Sr, and Ba and in Undoped Runs

Figure 10 presents D_ι's for other analyzed trace elements in order to address the question of whether doping with REE or Sr influences D_ι's of other trace elements at their natural concentration level. The position of a trace atom within a crystal structure has been discussed in the literature. In order to minimize near-order charge and size distortions caused by the substituting trace element, trace atoms have been proposed to form clusters with other trace atoms of a suitable size and charge to compensate for the poor fit of the trace atom into the crystal structure; even an embryonic phase consisting of several trace atoms has been proposed (Navrotsky, 1978; Urusov and Dudnikova, 1998). In particular, the small ion Li was cited as a potential candidate to compensate for charge and size (Moore and White, 1974).

We do not detect any influence on the presence or identity of doping elements on the partition coefficients of undoped elements (apart from the REE discussed above). Remarkably, this is true for elements with a variety of valences and ionic radii. This is especially clear for relatively abundant elements that are determined with high precision with the ion microprobe, such as Ti, Mg, Fe, K, Sr, and Ba.

Considering the doped elements Sr and Ba, we also see no difference in D_{Sr} between REE-doped, Sr-doped or undoped runs for several plagioclase compositions (e.g., Bindeman et al., 1998). This implies that from the ~800 ppm (natural) to up to 11,000 ppm (doped) level the partitioning behavior of Sr follows the same Henry's law constant. In one analyzed Ba-doped sample, we also found no D_{Ba} dependence on concentration or doping element (~100 ppm natural vs. 5500 ppm doped), confirming electron microprobe results of Drake (1972).

Electron microprobe analyses of undoped samples and those doped with Sr, Ba or REE, show that feldspars containing up to 0.5 wt.% (~0.3 mol%) of total REE remain stoichiometric

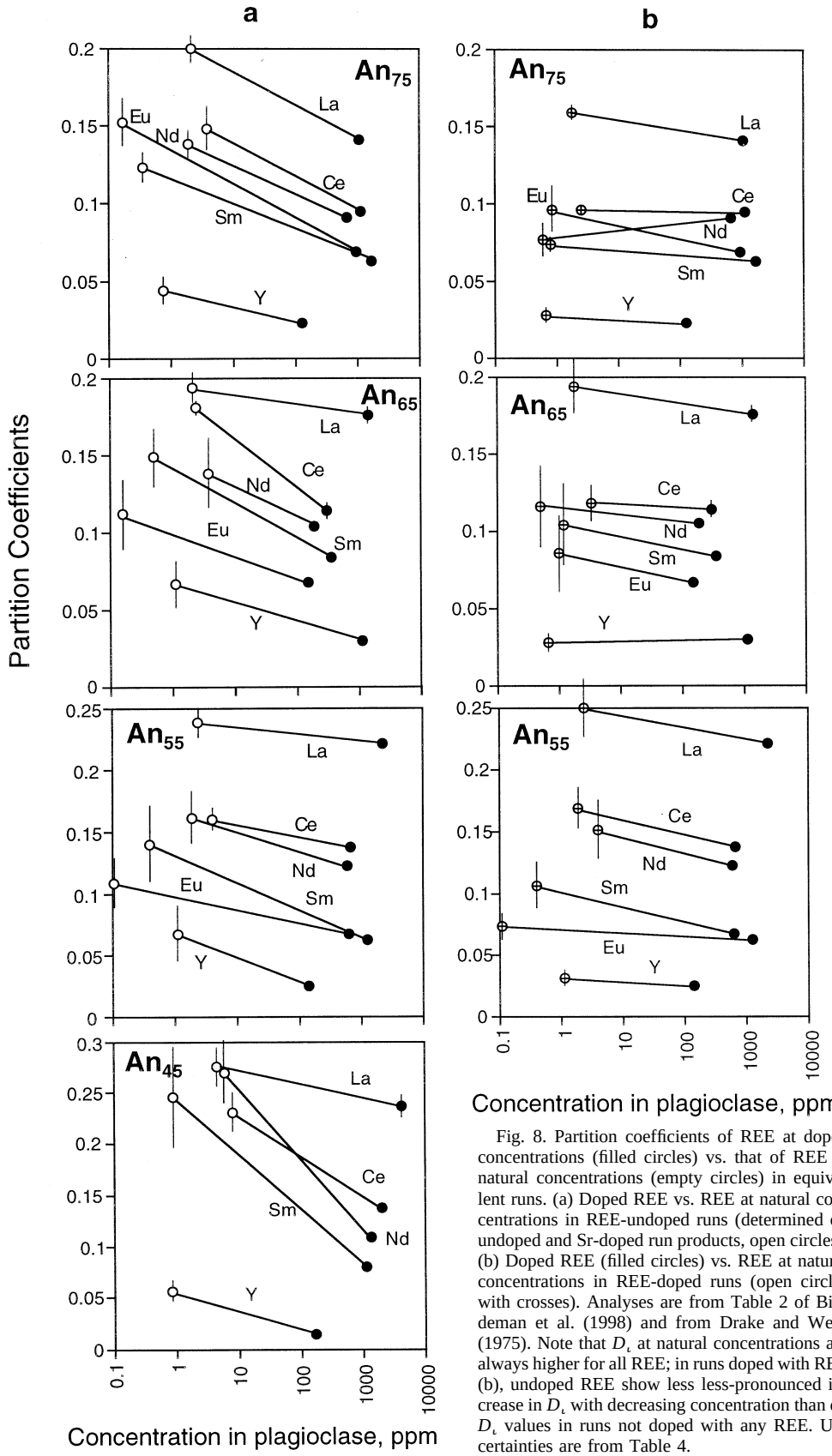

Fig. 8. Partition coefficients of REE at doped concentrations (filled circles) vs. that of REE at natural concentrations (empty circles) in equivalent runs. (a) Doped REE vs. REE at natural concentrations in REE-undoped runs (determined on undoped and Sr-doped run products, open circles). (b) Doped REE (filled circles) vs. REE at natural concentrations in REE-doped runs (open circles with crosses). Analyses are from Table 2 of Bindeman et al. (1998) and from Drake and Weill (1975). Note that D_i at natural concentrations are always higher for all REE; in runs doped with REE (b), undoped REE show less less-pronounced increase in D_i with decreasing concentration than do D_i values in runs not doped with any REE. Uncertainties are from Table 4.

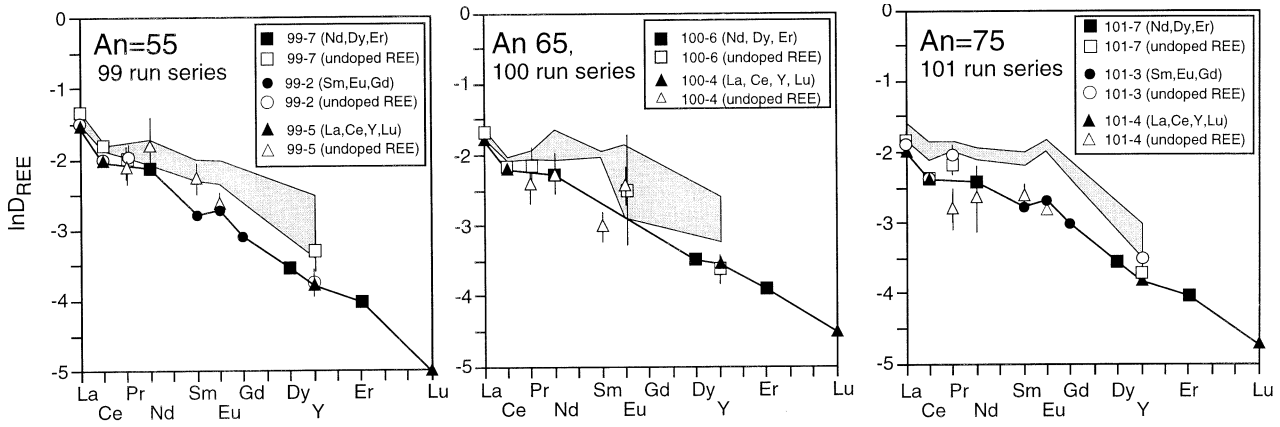

Fig. 9. Partition coefficients of doped and undoped REE and Y. Partition coefficients at natural concentration levels of REE measured on Sr-doped and undoped run series are shown as shadowed areas. Solid symbols indicate doped REE; corresponding open symbols indicate undoped REE. Note that undoped D_{REE}'s tend to cluster around doped D_{REE}'s in REE-doped run series.

within analytical accuracy (assuming that all these cations enter the *M* site). No feldspars were found to be deficient in *M*-site cations.

4. DISCUSSION

We observe that D_i's of analyzed trace elements other than REE are unaffected by the presence or identity of dopant elements. All other analyzed trace elements do not show any change in partitioning behavior as a result of doping with one, three, or even four different REE, Sr, or Ba. This argues against significant REE coupling with other trace elements in partitioning. It is improbable for a doped REE to encounter many monovalent trace elements in the vicinity of each trivalent REE atom to achieve a charge balance; the most likely monovalent

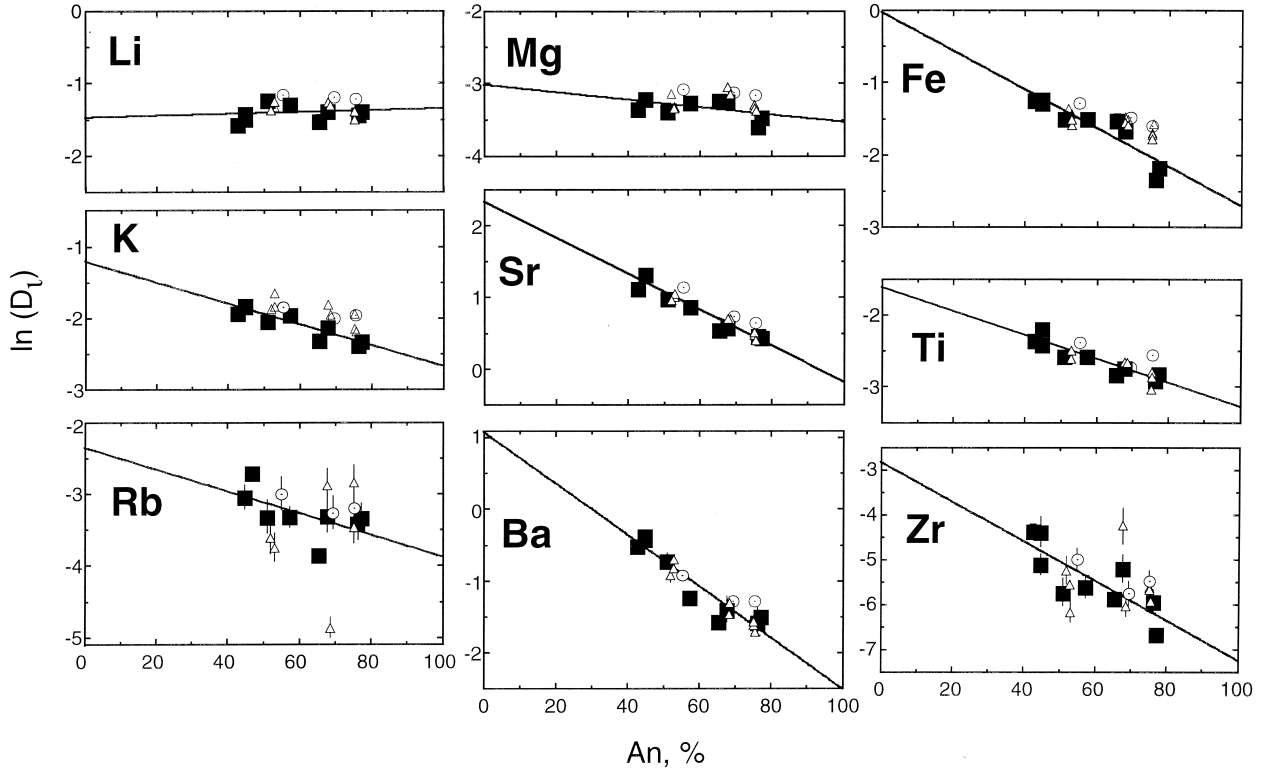

Fig. 10. Partition coefficients of trace elements between plagioclase and melt as a function of %An and doping element. Filled squares and solid regression lines are D_i determined earlier on Sr-doped samples (see Bindeman et al., 1998). Circles with dots are partition coefficients for undoped runs. Triangles are D_i for REE and Y-doped runs. Note that there is no difference in partition coefficients as a function of the doping element. We take this as the evidence against trace elements coupling between themselved in order to compensate for charge and size misfits of the dopant.

charge-balancing ion is Na^+, because of its much higher concentration. Therefore, major elements Ca and Na are the main participants in the exchange reactions with REE.

The difference in values between D_{REE} in undoped vs. those in REE-doped experiments (Figs. 7–9), suggests that the addition of wt.% of REE to the plagioclase-basalt system affects the D_ι's of REE and Y. Due to a geochemical similarity between different REE elements, adding selected REE changes (decreases) partition coefficients of *all* REE in these runs, even that of other undoped REE (e.g., Figs. 8b and 9). This may indicate that doping with REE leads to their partition into sites of similar size and charge that are suitable for REE and REE-like elements in plagioclase structure. The partition at doped concentration is structural and obeys predicted behavior for *M*-site partitioning (see Figs. 2, 5, and 6). However, partition at natural concentration level also obeys Onuma diagram with *M* site as a site of preferred substitution (see above and Bindeman et al., 1998). This implies that it is the plagioclase structure that is primarily responsible for the difference in D_ι's at different concentrations.

The partition coefficient D_ι of the plagioclase-melt trace element exchange reaction with a constant K can be expressed through the Henry's law constants of the trace element in the melt (κ_L) and plagioclase (κ_{Pl}) (e.g., Wood and Fraser, 1978):

$$D_\iota = K(\kappa_L)/(\kappa_{Pl}).$$

Because we consider equivalent experimental runs, K is expected to stay constant (for each exchange reaction). One explanation of higher D_ι's at natural concentrations is that adding a few wt.% of REE in the melt may cause a significant decrease in κ_L, thus affecting D_ι's. However, this is less likely since the heat of fusion of fictive REE-feldspar is much greater than the heat of its incorporation into the melt (e.g., Wood and Blundy, 1997). The other explanation, is that adding a few thousand of ppm of total REE to plagioclase increases κ_{Pl}, and, correspondingly, decreases D_{REE}'s. However, in a regular solution model of REE substitution for Ca and Na at magmatic temperatures, the REE–Ca interaction parameters are not expected to be more than 2–3 kcal/mole and a concentration change from ppm levels to 3 wt.% will produce less than a ~10% change in partition coefficients (e.g., Beattie, 1993). Therefore, in order for D_ι's at natural concentrations to be significantly larger (30–100%), different substitution mechanisms must be considered.

Feldspar synthesis studies demonstrate possible substitution mechanisms for trace elements in plagioclase. A variety of synthetic endmembers have been synthesized with B, Ga, Fe, Ni, Ge, Fe, Mg, and P entering the tetrahedral *T* site (Bychkov et al., 1989; Fleet et al., 1988; Galoisy and Calas, 1992), and Rb, NH_4, Tl, Sr, Ba, Pb, Eu, La (and other REE) in seven- to nine-coordinated *M* site (Kneip and Liebau, 1994; D'Arco and Piriou, 1989). For REE substitution, synthesis experiments and charge balance suggest that the following reactions operate:

$$2\,Ca^{2+} = REE^{3+} + Na^{1+}, \quad (1)$$

$$3\,Ca^{2+} = 2\,REE^{3+} + \text{vacancy}, \quad (2)$$

$$2\,Ca^{2+} = REE^{3+} + Trace^{1+}. \quad (3)$$

Substitution in the *M* site may be accompanied by the *T*-site substitutions:

$$Ca^{2+} + Al^{3+} = Na^{1+} + Si^{4+}, \quad (4)$$

$$Ca^{2+} + Si^{4+} = REE^{3+} + Al^{3+}. \quad (5)$$

A significant REE–Ca solid solution has been produced and demonstrates the feasibility of substitution mechanism (Eqn. 1). Substitution mechanism (Eqn. 5) was shown to be less likely due to the Al-tetrahedral avoidance rule, however Ismatov et al. (1985) synthesized REE-anorthite with Al/Si $>$ 1, which shows a limited possibility of this mechanism. Remarkably, the synthesized REE-bearing feldspar can tolerate a significant proportion of vacancies (Kimata, 1988; Kneip and Liebau, 1994), confirming the feasibility of substitution mechanism (Eqn. 2). We argued above against the possibility that exchange reactions with monovalent trace elements at natural concentration (Eqn. 3) serve as a mechanism of charge balancing of REE. Since we cannot detect stoichiometric deficiencies or excesses in Drake's experiments, we suggest that because the experiments used natural basalts, the availability of other trace and minor elements, such as Fe, Mg, and Ti, may compensate for vacancies (e.g., Watson, 1985).

In order to account for higher D_ι's at natural concentrations, we speculate that REE at natural concentrations may be involved in several substitution mechanisms (e.g., Eqns. 2 and 5), some of which can operate only at low concentrations. With the increase in REE concentrations, the low-concentration equilibria become saturated and the relative importance of mechanisms other than Eqn. 1 vanishes. In particular, defect equilibria (Eqn. 2) may be saturated and Al-avoidance does not allow reaction 5 to operate, at higher concentrations.

Urusov and Dudnikova (Eqn. 6, 1998) and Harrison and Wood (Eqn. 5, 1980) showed that when a defect equilibria are taken into account with a certain constant of the reaction, along with a heterovalent trace element exchange reaction, the D_ι is an algebraic function of two constants of these reactions. The resulting equations yield plateau of higher D_ι's at natural concentrations, and plateau of lower D_ι's at doped concentrations, and a narrow transition zone. We suggest that the same result can be derived not only for defect equilibria, but also for these exchange reactions operating at low concentrations, yielding two (or more) plateaus of D_{REE} as a function of REE concentration. The same may also be true for other trace elements, especially those involved in heterovalent substitution with several possible reactions, but this seems not to be the case with the homovalently substituting cations like Sr and Ba. Specifically designed experiments involving trace elements other than REE and conducted equivalently at doped and undoped concentrations may be necessary to clarify this question in the future.

We conclude that partition coefficients determined at natural concentration levels of trace elements of the present study and reported in Bindeman et al. (1998) are to be preferred for geochemical use. In this paper we discuss in details the role of REE-doping on decreasing D_{REE} by 30–100% and possible reasons for this effect. We emphasize that the natural range of concentrations of REE in plagioclase (tholeiites to alkali-rich pegmatites) is much smaller than that of doped experiments. Therefore, our D_{REE} measured at natural concentration levels

in experiments that are not doped with REE are most appropriate to use.

Acknowledgments—We are grateful to Professor M. J. Drake for providing samples of experiments for this study and for fruitful discussions and to J. D. Blundy for recommendations on the approximation technique. This work was supported by NASA Grant No. NAG5-4298 (to A.M.D.), and NSF Grant No. EAR 9417787 to A. T. Anderson.

REFERENCES

Angel R. J., Hazen R. M., McCormick T. C., Prewitt C. T., and Smyth J. R. (1988) Comparative compressibility of end-member feldspars. *Phys. Chem. Minerals* **15,** 313–318.

Beattie P. (1994) Systematics and energetics of trace-element partitioning between olivine and silicate melts: Implications for the nature of mineral/melt partitioning. *Chem. Geol.* **117,** 57–71.

Beattie P. (1993) The occurrence of apparent non-Henry's law behavior in experimental partitioning studies. *Geochim. Cosmochim. Acta* **57,** 47–55.

Bindeman I. N., Davis A. M., and Drake M. J. (1998) Ion microprobe study of plagioclase-basalt partition experiments at natural concentration level of trace elements. *Geochim. Cosmochim. Acta* **62,** 1175–1193.

Blundy J. D. and Wood B. J. (1994) Prediction of crystal-melt partition coefficients from elastic moduli. *Nature* **372,** 452–454.

Blundy J. D. and Wood B. J. (1991) Crystal-chemical control on the partitioning of Sr and Ba between plagioclase feldspar, silicate melts, and hydrothermal solutions. *Geochim. Cosmochim. Acta* **55,** 193–209.

Brice J. C. (1975) Some thermodynamic aspects of the growth of strained crystals. *J. Cryst. Growth* **28,** 249–253.

Bychkov A. M., Kotel'nikov A. R., Romanenko I. M., and Senderov E. E. (1989) Effect of isomorphic replacement of silicon by phosphorus on structural peculiarities of feldspars. *Geochem. Int.* **2,** 310–312.

D'Arco P. and Piriou B. (1989) Fluorescence spectra of Eu^{3+} in synthetic polycrystalline anorthite: distribution of Eu^{3+} in the structure. *Am. Min.* **74,** 191–199.

Drake M. J. (1972) Ph.D. dissertation, University of Oregon.

Drake M. J. and Holloway J. R. (1978) "Henry's law" behavior of Sm in a natural plagioclase/melt system: Importance of experimental procedure. *Geochim. Cosmochim. Acta* **42,** 679–683.

Drake M. J. and Weill D. F. (1975) Partition of Sr, Ba, Eu^{2+}, Eu^{3+}, and other REE between plagioclase feldspar and magmatic liquid: An experimental study. *Geochim. Cosmochim. Acta* **39,** 689–712.

Drake M. J. (1975) The oxidation state of europium as an indicator of oxygen fugacity. *Geochim. Cosmochim. Acta* **39,** 55–64.

Dudais M. J., Schmitt R. A., and Harward M. E. (1971) Trace element partitioning between volcanic plagioclase and dacitic pyroclastic matrix. *Earth Planet. Sci. Lett.* **11,** 440–446.

Dunn T. and Sen C. (1994) Mineral/matrix partition coefficients for orthopyroxene, plagioclase, and olivine in basaltic to andesitic systems: A combined analytical and experimental study. *Geochim. Cosmochim. Acta* **58,** 717–733.

Fleet M. E. (1988) Tetrahedral-site occupancies in reedmergnerite and synthetic boron albite ($NaBSi_3O_8$). *Am. Mineral.* **77,** 76–84.

Francalanci L. (1989) Trace element partition coefficients for minerals in shoshonitic and calc-alkaline rocks from Stromboli Island (Aeolian Arc). *Neues-Jahrbuch-fuer-Mineralogie, Abhandlungen.* **160,** 229–247.

Fujimaki H., Tatsumoto M., and Aoki K. (1984) Partition coefficients of Hf, Zr, and REE between phenocrysts and groundmasses. *J. Geophys. Res., (Suppl.)* **89,** B662–B672.

Galoisy L. and Calas G. (1992) Network forming nickel in feldspar. *Eos Trans.* **73,** 361.

Harrison W. and Wood B. J. (1980) An experimental investigation of the partitioning of REE between garnet and liquid with reference to the role of defect equilibria. *Contrib. Mineral. Petrol.* **72,** 145–155.

Higuchi H. and Nagasawa H. (1969) Partition of trace elements between rock forming minerals and host volcanic rocks. *Earth Planet. Sci. Lett.* **7,** 281–287.

Hinton R. W., Davis A. M., Scatena-Wachel D. E., Grossman L., and Draus R. J. (1988) A chemical and isotopic study of hibonite-rich refractory inclusions in primitive meteorites. *Geochim. Cosmochim. Acta* **52,** 2573–2598.

Hoover J. D. (1978) The distribution of samarium and tulium between plagioclase and liquid in the systems Di-An, Ab-An-Di at 1300°C. *Carnegie Inst. Wash. Yrbook.* **77,** 703–709.

Ismatov A. A., Yunusov M. Yu., and Nasyrova D. S. (1985) Solid solution of the composition $Ca_7TrAl_{17}Si_{15}O_{64}$ having the anorthite structure. *Inorganic Materials* **21,** 576–578.

Kimata M. (1988) The crystal structure of non-stoichiometric Eu-anorthite: an explanation of the Eu-positive anomaly. *Min. Mag.* **52,** 257–265.

Kneip H.-J. and Liebau F. (1994) Feldspars with trivalent non-tetrahedral cations: Experimental studies in the system $NaAlSi_3O_8$–$CaAl_2Si_2O_8$- $LaAl_3SiO_8$. *Eur. J. Min.* **6,** 87–98.

MacPherson G. J. and Davis A. M. (1994) Refractory inclusions in the prototypical CM chondrite, Mighei. *Geochim. Cosmochim. Acta* **58,** 5599–5625.

McKay G. A., Le L., Wagstaff J., and Crozaz G. (1994) Experimental partitioning of rare earth elements and strontium: constraints on petrogenesis and redox conditions during crystallization of Antarctic angrite Lewis Cliff 86010. *Geochim. Cosmochim. Acta* **58,** 2911–2919.

Moore R. J., and White J. (1974) Equilibrium relationships in the systems Li–Co–O and Li–Ni–O. *J. Mat. Sci.* **9,** 1401–1408.

Mysen B. O. (1978) Limits of solution of trace elements in minerals according to Henry's Law: Review of experimental data. *Geochim. Cosmochim. Acta* **42,** 871–885.

Nagasawa H. and Schnetzler C. C. (1971) Partitioning of rare earth, alkali, and alkali earth elements between phenocrysts and acidic igneous rocks. *Geochim. Cosmochim. Acta* **35,** 953–968.

Nash W. P. and Crecraft M. R. (1985) Partition coefficients for trace elements in silicic magmas. *Geochim. Cosmochim. Acta* **49,** 2309–2332.

Navrotsky A. (1978) Thermodynamics of element partitioning: (1) systematics of transition metals in crystalline and molten silicates and (2) defect chemistry and "the Henry's Law problem." *Geochim. Cosmochim. Acta* **42,** 887–902.

Onuma N., Higuchi H., Wakita H., and Nagasawa H. (1968) Trace element partition between two pyroxenes and host lava. *Earth Planet. Sci. Lett.* **5,** 47–51.

Peters M. T., Shaffer E. E., Burnett D. S., and Kim S. S. (1995) Magnesium and titanium partitioning between anorthite and Type B CAI liquid: Dependence on oxygen fugacity and liquid composition. *Geochim. Cosmochim. Acta* **59,** 2785–2796.

Petrov I., Agel A., and Hafner S. S. (1989a) Distinct defect centers at oxygen positions in albite. *Am. Mineral.* **74,** 1130–1341.

Petrov I., Bershov L. V., Hafner S. S., and Kroll H. (1989b) Order-disorder of Fe^{3+} ions over the tetrahedral positions in albite. *Am. Mineral.* **74,** 604–609.

Phinney W. C. (1992) Partition coefficients for iron between plagioclase and basalt as a function of oxygen fugacity; implication for Archean and lunar anorthosites. *Geochim. Cosmochim. Acta* **56,** 1885–1895.

Phinney W. C. and Morrison D. A. (1990) Partition coefficients for calcic plagioclase; implications for Archean anorthosites. *Geochim. Cosmochim. Acta* **54,** 1639–1654.

Schnetzler C. C. and Philpotts J. A. (1970) Partition coefficients of rare earth elements between igneous matrix material phenocrysts II. *Geochim. Cosmochim. Acta* **34,** 307–340.

Phinney W. C. and Morrison D. A. (1990) Partition coefficients for calcic plagioclase; implications for Archean anorthosites. *Geochim. Cosmochim. Acta* **54,** 1639–1654.

Schreiber H. D., Lauer H. V., Jr., and Thanyasiri T. (1980) The redox state of cerium in basaltic magmas: An experimental study of iron-cerium interactions in silicate melts. *Geochim. Cosmochim. Acta* **44,** 1599–1612.

Shannon R. D. (1976) Revised effective ionic radii and systematic studies of interatomic distances in halides and chalcogenides. *Acta Crystallogr.* **A32,** 751–767.

Simon S. B., Kuehner S. M., Davis A. M., Grossman L., Johnson M. L., and Burnett D. S. (1994) Experimental studies of trace element

partitioning in Ca, Al-rich compositions: Anorthite and perovskite. *Geochim. Cosmochim. Acta* **58,** 1507–1523.

Urusov V. S. and Dudnikova V. B. (1998) The trace-component trapping effect: Experimental evidence, theoretical interpretation, and geochemical applications. *Geochim. Cosmochim. Acta* **62,** 1233–1240.

Urusov V. S. and Kravchuk I. F. (1978) Trapping effect of microimpurity by the defect sites and its geochemical significance. *Geochem. Int.* **N7,** 963–978.

Vernieres J., Joron J.-L., Treuil M., Coulon C., and Dupuy C. (1977) Coefficient de partage de quelques elements en trace entre plagioclase et verre dans les ignimbrites—Implications petrogenetiques. *Chem. Geol.* **19,** 309–325.

Watson E. B. (1985) Henry's Law behavior in simple systems and in magmas: Criteria for discerning concentration-dependent partition coefficients in nature. *Geochim. Cosmochim. Acta* **49,** 917–923.

Watson E. B. and Harrison T. M. (1984) Accessory minerals and the geochemical evolution of crustal magma systems: A summary and prospectus of experimental approaches. *Phys. Earth Planet. Int.* **35,** 19–30.

Wilke M. and Behrens H. (1999) The dependence of the partitioning of iron and europium between plagioclase and hydrous tonalitic melt on oxygen fugacity. *Contrib. Mineral. Petrol.* **137,** 102–114.

Williamson J. H. (1968) Least-squares fitting of a straight line. *Can. J. Phys.* **46,** 1845–1854.

Wood B. J. and Blundy J. D. (1997) A predictive model for rare earth element partitioning between clinopyroxene and anhydrous silicate melt. *Contrib. Mineral. Petrol.* **129,** 166–181.

Wood B. J. and Fraser D. G. (1978) *Elementary Thermodynamics for Geologists*. Oxford University Press, 303 p.

Worner G., Beusen J. M., Duchateau N., Gijbels R., and Schmincke H.-U. (1983) Trace element abundances and mineral/melt distribution coefficients in Laacher See Volcano (Germany). *Contrib. Mineral. Petrol.* **84,** 152–173.